# Infrared behavior of the gluon propagator in nonequilibrium situations

Fred Cooper*
*T-8, Theoretical Division, Los Alamos National Laboratory, Los Alamos, New Mexico 87545*

Chung-Wen Kao†
*Theoretical Physics Group, Department of Physics and Astronomy, University of Manchester, Manchester M139PL, United Kingdom*

Gouranga C. Nayak‡
*T-8, Theoretical Division, Los Alamos National Laboratory, Los Alamos, New Mexico 87545*
(Received 4 April 2002; published 30 December 2002)

The infrared behavior of the medium modified gluon propagator in nonequilibrium situations is studied in the covariant gauge using the Schwinger-Keldysh closed-time path formalism. It is shown that the magnetic screening mass is nonzero at the one loop level whenever the initial gluon distribution function is nonisotropic with the assumption that the distribution function of the gluon is not divergent at zero transverse momentum. For isotropic gluon distribution functions, such as those describing local equilibrium, the magnetic mass at the one loop level is zero, which is consistent with finite temperature field theory results. Assuming that a reasonable initial gluon distribution function can be obtained from a perturbative QCD calculation of minijets, we determine these out of equilibrium values for the initial magnetic and Debye screening masses at energy densities appropriate to BNL RHIC and CERN LHC. We also compare the magnetic masses obtained here with those obtained using finite temperature lattice QCD methods at similar temperatures at RHIC and LHC.

DOI: 10.1103/PhysRevD.66.114016 PACS number(s): 12.38.Cy, 11.10.Wx, 12.38.Mh

Experiments at the BNL Relativistic Heavy Ion Collider (RHIC) (Au-Au collisions at $\sqrt{s}=200$ GeV) and CERN Large Hadron Collider (LHC) (Pb-Pb collisions at $\sqrt{s}=5.5$ TeV) will provide an excellent opportunity to produce a quark-gluon plasma in the laboratory. There is no doubt that an energy density larger than $\sim 5$ GeV/fm$^3$ [1] will be created during these collisions but it is not at all clear that the partons produced following the collision will reach equilibrium. The study of the equilibration of the quark-gluon plasma is very crucial because it determines the time evolution of all global quantities such as energy density, number density, etc. This study also plays a crucial role in determining many of the potential signatures for quark-gluon plasma detection at RHIC. The space-time evolution of the parton gas for this nonequilibrium situation can be be modeled by solving semiclassical relativistic transport equations [2–10]. Central to solving the transport equations is what goes into the scattering kernels. Perturbative vacuum expressions for gluon scattering suffer from severe infrared problems. One loop medium effects in equilibrium provide an electric (Debye) screening mass, but not a magnetic screening mass [11]. Thus one cannot use a one loop resummed finite temperature gluon propagator as an approximation to the scattering kernel because of severe infrared problems in the limit that $p_0=0$ and $|\vec{p}|\to 0$. To obtain magnetic screening in equilibrium situations requires a nonperturbative lattice QCD calculation. What we would like to point out here is that if we use the $CTP$ formalism [12] with an *arbitrary* nonthermal initial Gaussian density matrix then it is possible to obtain at one loop a magnetic screening mass as long as the initial gluon single particle distribution function $f(k_x,k_y,k_z,t_0)$ is not isotropic with the assumption that the gluon distribution function is not divergent at zero transverse momentum. That is, we assume that at $t=t_0$ one can write a Fourier decomposition of the gluon field in terms of creation and annihilation operators. By a Bogoliubov transformation at $t=t_0$ one can always set the pair distribution functions $\langle a^\dagger_\lambda(\vec{k},t=t_0)a^\dagger(\vec{q},t=t_0)_\lambda\rangle=\langle a_\lambda(\vec{k},t=t_0)a(\vec{q},t=t_0)_\lambda\rangle=0$. Thus the propagator will have the usual vacuum part and a term which depends on the initial expectation value of the number density

$$\sum_{\lambda=1}^{2}\langle a^\dagger_\lambda(\vec{k},t=t_0)a(\vec{q},t=t_0)_\lambda\rangle = f(\vec{k},t_0)(2\pi)^3\delta(\vec{k}-\vec{q}), \tag{1}$$

and we have summed over the physical transverse polarizations. For $f$ to correspond to a physically realizable quantity the number density as well as energy density has to be finite. Thus $f(\vec{k},t)$ has to go to zero as $k\to\infty$ fast enough so that one obtains finite number density and energy density. For Gaussian initial value problems, one only needs to know the two-point function at $t=t_0$. In our following analysis, we will also need to make a quasi-adiabatic approximation so that we will assume, for the purpose of determining the initial screening masses, that the system is time-translation invariant. Thus the only difference we will assume in our Green's functions from the usual thermal ones will be the choice of an anisotropic $f(\vec{k},t_0)$ which will replace the usual Bose-Einstein distribution function. This approximation has

*Electronic address: fcooper@lanl.gov
†Electronic address: kao@a35.ph.man.ac.uk
‡Electronic address: nayak@shakti.lanl.gov

 

been discussed in detail by Thoma and others [13]. In our calculations, we will use a simple ansatz for $f(\vec{k},t_0)$ in which the parameters will be chosen to agree with known distributions for minijet production at RHIC and LHC. Here we are not suggesting that this effect replaces the nonperturbative magnetic screening mass, but that the effect we are considering is of the same order of magnitude and already cures the infrared problems of the transport theory.

In what follows we will examine the infrared behavior of the medium modified gluon propagator at one loop using the $CTP$ formalism. The purpose of this paper is to study the static limit of the longitudinal and transverse self-energy of the gluon (Debye and magnetic screening masses) and, in particular, to determine, at the one loop level, how the magnetic screening mass depends on the initial $f(\vec{k},t_0)$. Although technically the magnetic screening mass is defined as the position of the zero of the inverse propagator [i.e. in the limit $p_0=0,|\vec{p}|\to m_{sc}, m_{sc}^2=\Pi(m_{sc}^2)$] [14], at one loop the limit of the inverse propagator as $p_0=0,|\vec{p}|\to 0$ *is* gauge invariant (independent of $\xi$ for general covariant $\xi$ gauges), and moreover this limit is the one important for controlling the infrared properties of the collision kernel in the transport theory. Thus in this paper we will use the second limiting process to define the screening masses. At arbitrary momentum the polarization is not in general gauge invariant at one loop. To have a gauge invariant approximation at one loop one can make a hard momentum loop approximation as discussed in [13,15].

In particular we are interested in nonisotropic nonthermal forms for $f(\vec{k},t_0)$ consistent with known minijet production results. Let us consider an expanding system of partons in $1+1$ dimensions. For this purpose we introduce the flow velocity of the medium:

$$u^\mu=(\cosh\eta,0,0,\sinh\eta), \tag{2}$$

where $\eta=\frac{1}{2}\ln(t+z)/(t-z)$ is the space-time rapidity and $u_\mu u^\mu=1$. We define the four symmetric tensors [16–18] as

$$T_{\mu\nu}(p)=g_{\mu\nu}-\frac{(u\cdot p)(u_\mu p_\nu+u_\nu p_\mu)-p_\mu p_\nu-p^2u_\mu u_\nu}{(u\cdot p)^2-p^2},$$

$$L_{\mu\nu}(p)=\frac{-p^2}{(u\cdot p)^2-p^2}\left(u_\mu-\frac{(u\cdot p)p_\mu}{p^2}\right)\left(u_\nu-\frac{(u\cdot p)p_\nu}{p^2}\right),$$

$$C_{\mu\nu}(p)=\frac{1}{\sqrt{2[(u\cdot p)^2-p^2]}}\times\left[\left(u_\mu-\frac{(u\cdot p)p_\mu}{p^2}\right)p_\nu+\left(u_\nu-\frac{(u\cdot p)p_\nu}{p^2}\right)p_\mu\right],$$

$$D_{\mu\nu}(p)=\frac{p_\mu p_\nu}{p^2}. \tag{3}$$

Here $T^{\mu\nu}$ is transverse with respect to the flow-velocity but $L^{\mu\nu}$ and $D^{\mu\nu}$ are mixtures of space-like and time-like components. These tensors satisfy the following transversality properties with respect to $p^\mu$:

$$p_\mu T^{\mu\nu}(p)=p_\mu L^{\mu\nu}(p)=0,$$

$$p_\mu p_\nu C^{\mu\nu}(p)=0. \tag{4}$$

In terms of this tensor basis the gluon propagator in the covariant gauge is given by

$$\tilde{G}_{\mu\nu}(p)=-iT_{\mu\nu}(p)\tilde{G}^T(p)-iL_{\mu\nu}(p)\tilde{G}^L(p)-i\xi D_{\mu\nu}(p)\tilde{G}^D(p), \tag{5}$$

where $\tilde{G}^T$, $\tilde{G}^L$, $\tilde{G}^D$ correspond to $T$, $L$ and $D$ components respectively of the full gluon propagator at the one loop level. The last part $\tilde{G}^D(p)$ is identical to the vacuum part [16] and hence we do not consider it anymore. There are separate Dyson-Schwinger equations for the different components of the $CTP$ matrix Green's functions that do not couple with each other. These equations can be written in the form

$$[\tilde{G}^{T,L}(p)]_{ij}=[G^{T,L}(p)]_{ij}+\sum_{l,k}[G^{T,L}(p)]_{il}\times[\Pi^{T,L}(p)]_{lk}\cdot[\tilde{G}^{T,L}(p)]_{kj}. \tag{6}$$

Here $i,j,k,l=+,-$ are the $CTP$ contour labels, and suppression of Lorentz and color indices in the above equation is understood.

In the Keldysh rotated representation of the $CTP$ formalism, in terms of retarded, advanced and symmetric Green's functions we have instead

$$\tilde{G}^{T,L}_{R,A}(p)=G^{T,L}_{R,A}(p)+G^{T,L}_{R,A}(p)\cdot\Pi^{T,L}_{R,A}(p)\cdot\tilde{G}^{T,L}_{R,A}(p). \tag{7}$$

The straightforward solution of the above equation is given by

$$\tilde{G}^{T,L}_{R,A}(p)=\frac{G^{T,L}_{R,A}(p)}{1-G^{T,L}_{R,A}(p)\cdot\Pi^{T,L}_{R,A}(p)}=\frac{1}{p^2-\Pi^{T,L}_{R,A}(p)\pm i\,\mathrm{sgn}(p_0)\epsilon}, \tag{8}$$

where the self-energy contains the medium effects. Similar but more complicated equations are obtained for the resummed symmetric Green's functions

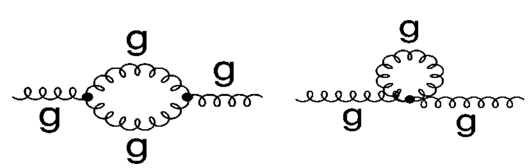


FIG. 1. One loop graphs for the gluon self-energy.

$$\tilde{G}_S^{T,L}(p)=[1+2f(\vec{p})]\mathrm{sgn}(p_0)[\tilde{G}_R^{T,L}(p)-\tilde{G}_A^{T,L}(p)]+\{\Pi_S^{T,L}(p)-[1+2f(\vec{p})]\mathrm{sgn}(p_0)[\Pi_R^{T,L}(p)-\Pi_A^{T,L}(p)]\}\tilde{G}_R^{T,L}(p)\times\tilde{G}_A^{T,L}(p). \tag{9}$$

For the purposes of obtaining the correct kernel for the Boltzmann equation, we need the medium improved Feynman propagator for the gluon at the one loop level which is just one component $\{++\}$ of the matrix Green's function of the $CTP$ formalism.

$G_F(p)\equiv[\tilde{G}(p)]_{++}$ can be written as

$$[\tilde{G}(p)]_{++}=\frac{1}{2}[\tilde{G}_S(p)+\tilde{G}_A(p)+\tilde{G}_R(p)], \tag{10}$$

where $G_A, G_R, G_S$ stand for advanced, retarded and symmetric Green's function respectively. In the above equation the "$+$" sign refers to the upper branch in the closed-time path. Using the relations of the various self-energies one finds [13,15]

$$\tilde{G}_{++}(p)=\frac{p^2-\mathrm{Re}\,\Pi_R(p)+\frac{1}{2}\mathrm{Im}\,\Pi_S(p)}{[p^2-\mathrm{Re}\,\Pi_R(p)]^2+[\mathrm{Im}\,\Pi_R(p)]^2}, \tag{11}$$

where $\mathrm{Re}\,\Pi_R(p)$ and $\mathrm{Im}\,\Pi_R(p)$ are the real and imaginary part of the retarded self-energy. These self-energies have both longitudinal and transverse parts which, in the static limit $(p_0=0,|\vec{p}|\to 0)$, give Debye and magnetic screening masses of the gluon respectively. In the above equation $\Pi_S(p)$ is the symmetric part of the self-energy.

To obtain the infrared behavior of this propagator we need to find the static limit of the gluon self-energy for an anisotropic $f(\vec{k},t)$ corresponding to the initial distribution function expected from the parton model. In a frozen ghost formalism [18,19], the gluon self-energy is obtained from the gluon loop and tadpole loop as shown in Fig. 1. The ghost does not contribute to the medium effect in this formalism because the initial density of states is chosen to be that of the physical gluons. All the effects of the ghost are present in the vacuum.

The general expressions for the real and imaginary part of the gluon self-energy in nonequilibrium in a covariant gauge for an expanding gluonic medium have been derived in a previous paper [15]. Here we examine the static limit of these self-energies which play crucial roles to obtain a finite collision integral to study equilibration of the quark-gluon plasma at RHIC and LHC. The general expressions for the real part of the longitudinal and transverse self-energy of the gluon loop are given by

$$\mathrm{Re}\,\Pi^L_{Gl;R}(p)=\frac{g^2}{2}\delta_{ab}N_c\int\frac{d^3q}{(2\pi)^3}\Bigg[\frac{1}{2|\vec{q}|}\{[f(\vec{q})G(q,p)]_{q^0=|\vec{q}|}+[f(-\vec{q})G(q,p)]_{q^0=-|\vec{q}|}\}+\frac{1}{2|\vec{p}-\vec{q}|}\{[f(\vec{p}-\vec{q})G(p-q,p)]_{p^0-q^0=|\vec{p}-\vec{q}|}+[f(-\vec{p}+\vec{q})G(p-q,p)]_{p^0-q^0=-|\vec{p}-\vec{q}|}\}\Bigg] \tag{12}$$

and

$$\mathrm{Re}\,\Pi^T_{Gl;R}(p)=\frac{g^2}{2}\delta_{ab}N_c\int\frac{d^3q}{(2\pi)^3}\Bigg[\frac{1}{2|\vec{q}|}\{[f(\vec{q})H(q,p)]_{q^0=|\vec{q}|}+[f(-\vec{q})H(q,p)]_{q^0=-|\vec{q}|}\}+\frac{1}{2|\vec{p}-\vec{q}|}\{[f(\vec{p}-\vec{q})H(p-q,p)]_{p^0-q^0=|\vec{p}-\vec{q}|}+[f(-\vec{p}+\vec{q})H(p-q,p)]_{p^0-q^0=-|\vec{p}-\vec{q}|}\}\Bigg] \tag{13}$$

where

$$G(q,p)=\frac{1}{(p^0-q^0)^2-(\vec{p}-\vec{q})^2}\Bigg\{\frac{8p^2}{(u\cdot p)^2-p^2}\Bigg[\left((u\cdot q)-\frac{(u\cdot p)(q\cdot p)}{p^2}\right)^2\Bigg]-[(p+q)^2]\Bigg[\frac{2(q\cdot p)(p\cdot u)^3}{(q\cdot u)p^2[(p\cdot u)^2-p^2]}-\frac{(q\cdot p)^2(p\cdot u)^2}{(q\cdot u)^2p^2[(p\cdot u)^2-p^2]}-\frac{(p\cdot u)^2}{[(p\cdot u)^2-p^2]}\Bigg]-4p^2+8\frac{(q\cdot p)(u\cdot p)}{(u\cdot q)}-4\frac{(q\cdot p)^2}{(u\cdot q)^2}+(\xi-1)\frac{(p\cdot u)^2[(q\cdot p)^2-2(q\cdot u)(p\cdot u)(q\cdot p)+(q\cdot u)^2p^2]}{(q\cdot u)^2[p^2-(p\cdot u)^2]}\Bigg\} \tag{14}$$

and

$$H(q,p)=\frac{1}{(p^0-q^0)^2-(\vec{p}-\vec{q})^2}\Bigg\{8\frac{(u\cdot q)(q\cdot p)(u\cdot p)}{(u\cdot p)^2-p^2}-4\frac{(q\cdot p)^2}{(u\cdot p)^2-p^2}-4\frac{p^2(q\cdot u)^2}{(u\cdot p)^2-p^2}-[(p+q)^2]\Bigg[1-\frac{(q\cdot p)(u\cdot p)}{(u\cdot q)[(u\cdot p)^2-p^2]}$$
$$+\frac{(q\cdot p)^2}{2(u\cdot q)^2[(u\cdot p)^2-p^2]}+\frac{p^2}{2[(u\cdot p)^2-p^2]}\Bigg]-4p^2+8\frac{(q\cdot p)(u\cdot p)}{(u\cdot q)}-4\frac{(q\cdot p)^2}{(u\cdot q)^2}$$
$$+\frac{(\xi-1)(p^4\{-(q\cdot p)^2+2(q\cdot u)(p\cdot u)(q\cdot p)+(q\cdot u)^2[p^2-2(p\cdot u)^2]\})}{2(q\cdot u)^2[(q\cdot p)-p^2][p^2-(p\cdot u)^2]}\Bigg\}. \tag{15}$$

The general expression for the tadpole loop contribution is given by

$$\Pi^L_{Ta;R}(p)=g^2\delta_{ab}N_c\int\frac{d^3q}{(2\pi)^3}\frac{f(\vec{q})}{2|\vec{q}|}\left[3-2\frac{(u\cdot p)(q\cdot p)}{p^2(u\cdot q)}+\frac{p^2}{(u\cdot p)^2-p^2}\left(1-\frac{(u\cdot p)(q\cdot p)}{p^2(u\cdot q)}\right)^2\right]\Bigg|_{q_0=|\vec{q}|}$$
$$+\frac{f(-\vec{q})}{2|\vec{q}|}\left[3-2\frac{(u\cdot p)(q\cdot p)}{p^2(u\cdot q)}+\frac{p^2}{(u\cdot p)^2-p^2}\left(1-\frac{(u\cdot p)(q\cdot p)}{p^2(u\cdot q)}\right)^2\right]\Bigg|_{q_0=-|\vec{q}|} \tag{16}$$

and

$$\Pi^T_{Ta;R}(p)=g^2\delta_{ab}N_c\int\frac{d^3q}{(2\pi)^3}\frac{f(\vec{q})}{2|\vec{q}|}\left[1+\frac{(u\cdot p)(q\cdot p)}{(u\cdot q)[(u\cdot p)^2-p^2]}-\frac{(q\cdot p)^2}{2(u\cdot q)^2[(u\cdot p)^2-p^2]}-\frac{p^2}{2[(u\cdot p)^2-p^2]}\right]\Bigg|_{q_0=|\vec{q}|}$$
$$+\frac{f(-\vec{q})}{2|\vec{q}|}\left[1+\frac{(u\cdot p)(q\cdot p)}{(u\cdot q)[(u\cdot p)^2-p^2]}-\frac{(q\cdot p)^2}{2(u\cdot q)^2[(u\cdot p)^2-p^2]}-\frac{p^2}{2[(u\cdot p)^2-p^2]}\right]\Bigg|_{q_0=-|\vec{q}|}. \tag{17}$$

To simplify these equations in the infrared limit we expand $f(\vec{q}-\vec{p})$ as $f(\vec{q}-\vec{p})=f(\vec{q})-\vec{p}\cdot\vec{\nabla}_q f(\vec{q})$ and neglect the higher order gradients. Similarly we expand $|\vec{p}-\vec{q}|$ as $|\vec{p}-\vec{q}|=|\vec{q}|\{1-(p\cdot\hat{q})/|\vec{q}|\}$. In the static limit (first taking $p_0=0$ then using $|\vec{p}|\to 0$), and in the rest frame ($u_0=1,\vec{u}=0$) we obtain from Eq. (12)

$$\mathrm{Re}\,\Pi^L_{Gl;R}(p_0=0,|\vec{p}|\to 0)=-2g^2\delta_{ab}N_c\left[\int\frac{d^3q}{(2\pi)^3}\left(\frac{\hat{p}\cdot\nabla_q f(\vec{q})}{\hat{p}\cdot\hat{q}}\right)+\int\frac{d^3q}{(2\pi)^3}\frac{f(\vec{q})}{|\vec{q}|}\right] \tag{18}$$

and from Eq. (16)

$$\Pi^L_{Ta;R}(p_0=0)=2g^2\delta_{ab}N_c\int\frac{d^3q}{(2\pi)^3}\frac{f(\vec{q})}{|\vec{q}|}. \tag{19}$$

Adding both the above equations we get the expression for the Debye screening mass,

$$m_D^2=[\mathrm{Re}\,\Pi^L_{Gl;R}(p_0=0,|\vec{p}|\to 0)]+[\mathrm{Re}\,\Pi^L_{Ta;R}(p_0=0,|\vec{p}|\to 0)]=-6g^2\int\frac{d^3q}{(2\pi)^3}\left(\frac{\hat{p}\cdot\nabla_q f(\vec{q})}{\hat{p}\cdot\hat{q}}\right) \tag{20}$$

which is the real part of the longitudinal self-energy. $N_C=3$ is used. This equation was obtained by various authors [20]. Similarly in the static limit and in the rest frame we get from Eq. (13)

$$\mathrm{Re}\,\Pi^T_{Gl;R}(p_0=0,|\vec{p}|\to 0)=g^2\delta_{ab}N_c\int\frac{d^3q}{(2\pi)^3}\left\{\frac{f(\vec{q})}{|\vec{q}|}\cdot\left[\frac{3}{2}(\hat{q}\cdot\hat{p})^2-\frac{1}{2}\right]+\frac{\hat{p}\cdot\nabla_q f(\vec{q})}{\hat{p}\cdot\hat{q}}\cdot[1-(\hat{q}\cdot\hat{p})^2]\right\} \tag{21}$$

and from Eq. (17)

$$\Pi^T_{Ta;R}(p_0=0)=g^2\delta_{ab}N_c\int\frac{d^3q}{(2\pi)^3}\frac{f(\vec{q})}{|\vec{q}|}\cdot\left[\frac{3}{2}-\frac{1}{2}(\hat{q}\cdot\hat{p})^2\right]. \tag{22}$$

Adding both the above equations we get the expression for the magnetic screening mass

$$m_g^2=[\mathrm{Re}\,\Pi^T_{Gl,R}(p_0=0,|\vec{p}|\to 0)]+[\mathrm{Re}\,\Pi^T_{Ta,R}(p_0=0,|\vec{p}|\to 0)]=3g^2\int\frac{d^3q}{(2\pi)^3}\left[\frac{f(\vec{q})}{|\vec{q}|}\cdot[1+(\hat{q}\cdot\hat{p})^2]+\frac{\hat{p}\cdot\nabla_q f(\vec{q})}{\hat{p}\cdot\hat{q}}\cdot[1-(\hat{q}\cdot\hat{p})^2]\right] \tag{23}$$

which is the real part of the transverse self-energy. For the imaginary part of the gluon self-energy at one loop we get $\mathrm{Im}\,\Pi^{T,L}_{GL:R}=0$, in the static limit. Note that the above formula uses the medium part of the self-energy containing a gluon loop and a tadpole loop which appears in the resummed gluon propagator [Eq. (11)]. The expression for the Debye screening mass that we obtained [see Eq. (20)] is the same as that obtained by various authors [20]. The expression we obtain here for the magnetic mass for a nonequilibrium gluon distribtution function is new [see Eq. (23)]. There is no approximation present in the derivation of Eqs. (20) and (23). The static limit results are gauge invariant.

For an isotropic gluon distribution function $f(|\vec{q}|)$ we get, from Eq. (20),

$$m_D^2=\frac{6g^2}{\pi^2}\int dq\,q\,f(q) \tag{24}$$

where $q=|\vec{q}|$ and from Eq. (23)

$$m_g^2=0. \tag{25}$$

Furthermore for the special isotropic case when the system is described by an equilibrium Bose-Einstein distribution function for the gluon, Eqs. (20) and (23) give

$$m_D^2=g^2T^2 \quad \text{and} \quad m_g^2=0 \tag{26}$$

respectively. These results [Eq. (26)] are identical to those obtained by using finite temperature field theory in QCD assuming that the system is in thermal equilibrium [11,17,21]. It is interesting to note that the magnetic mass is not only zero at the one loop level in equilibrium [Eq. (26)] but it is also zero for any isotropic nonequilibrium gluon distribution function [see Eq. (25)]. Only when the distribution function is nonisotropic does one get a nonzero contribution to the magnetic screening mass with the assumption that the distribution function of the gluon is not divergent at zero transverse momentum (see below). This result is not particular to QCD but also will be true for QED when the distribution function is nonisotropic. This is explicitly calculated in [22] for the QED case where we have shown that we get the exact same formula for the magnetic screening mass in QED as we obtained in this paper for QCD (gluon loop) except that $N_c g^2 \propto e^2$.

Before considering the situation at RHIC and LHC let us consider an example where there is momentum anisotropy in the transverse and longitudinal momentum distribution. For this purpose we work in the cylindrical coordinate system: $(q_t,\phi,q_z)$. From Eq. (20) we get

$$m_D^2=-\frac{6g^2}{(2\pi)^3}\int d^2q_t\int dq_z|\vec{q}|\left(\frac{\hat{p}\cdot\nabla_q f(\vec{q})}{\hat{p}\cdot\vec{q}}\right). \tag{27}$$

From this equation we realize that when $f(\vec{q})$ is isotropic, the dependence on $\hat{p}$ drops out and we obtain Eq. (24). For anisotropic $f$ the mass depends on the direction of $\hat{p}$. In what follows we will assume $\hat{p}$ is along the transverse direction and give values only for this direction. Similar results can be obtained for the longitudinal choice. Assuming $\hat{p}$ is along the transverse direction we find

$$m_{Dt}^2=-\frac{6g^2}{(2\pi)^3}\int dq_t\int d\phi\int dq_z\sqrt{q_t^2+q_z^2}\frac{\partial f(q_t,\phi,q_z)}{\partial q_t}. \tag{28}$$

Integrating by parts in $q_t$ we get

$$m_{Dt}^2=\frac{3g^2}{4\pi^3}\left[\int dq_t q_t\int d\phi\int\frac{dq_z}{|\vec{q}|}f(q_t,\phi,q_z)+\int d\phi\int dq_z[|q_z|f(q_t,q_z,\phi)]_{q_t=0}\right]. \tag{29}$$

For an equilibrium distribution function of the form $f_{eq}=1/(e^{\sqrt{q_x^2+q_y^2+q_z^2}/T}-1)=1/(e^{\sqrt{q_t^2+q_z^2}/T}-1)$ we get from the above equation

$$m_{Dt}^2=\frac{g^2T^2}{2}+\frac{g^2T^2}{2}=g^2T^2 \tag{30}$$

which is the correct result obtained by using finite temperature QCD.

Similarly, changing to a $q_t,\phi,q_z$ coordinate system we get from Eq. (23)

$$m_g^2=\frac{3g^2}{8\pi^3}\int dq_t q_t\int d\phi\int dq_z\left\{\frac{f(\vec{q})}{|\vec{q}|}\cdot\left[1+\frac{(\vec{q}\cdot\hat{p})^2}{|\vec{q}|^2}\right]+|\vec{q}|\frac{\hat{p}\cdot\nabla_q f(\vec{q})}{\hat{p}\cdot\vec{q}}\cdot\left[1-\frac{(\vec{q}\cdot\hat{p})^2}{|\vec{q}|^2}\right]\right\} \tag{31}$$

when $\hat{p}$ points in the transverse direction and we again perform partial integration over $q_t$ to obtain

$$m_{gt}{}^2=\frac{3g^2}{8\pi^3}\left[2\int dq_t q_t\int d\phi\cos^2\phi\int dq_z\frac{f(q_t,q_z,\phi)}{|\vec{q}|}-\int d\phi\int dq_z[|q_z|f(q_t,q_z,\phi)]_{q_t=0}\right]. \tag{32}$$

For an equilibrium distribution function of the form $f_{eq}=1/(e^{\sqrt{q_x^2+q_y^2+q_z^2}/T}-1)=1/(e^{\sqrt{q_t^2+q_z^2}/T}-1)$ the above equation gives

$$m_{gt}{}^2=\frac{3g^2}{(2\pi)^3}\left[(4\pi)\frac{\pi^2T^2}{6}-(4\pi)\frac{\pi^2T^2}{6}\right]=0, \tag{33}$$

which is consistent with finite temperature QCD results.

Before proceeding to compute the initial magnetic screening mass at RHIC and LHC situations we will adopt a nonisotropic test distribution function to compute the magnetic screening mass from the formula given by Eq. (32). We choose a nonisotropic test distribution function of the form

$$f=\frac{1}{e^{\sqrt{q_t^2+hq_z^2}/T}-1} \tag{34}$$

where $h$ is a parameter for nonisotropy. For $h=1$ we get the usual Bose-Einstein distribution function. Using the above nonisotropic distribution function we plot the magnetic screening mass from Eq. (32) in Fig. 2. It can be seen from Fig. 2 that for $h=1$ (corresponding to the Bose-Einstein distribution function) we get $m_{gt}=0$ and for $h\neq 1$ (corresponding to the nonisotropic distribution function) we get a nonzero magnetic screening mass.

Now we consider the realistic situation at RHIC and LHC. For the situation at RHIC and LHC where the parton distribution function at $t=t_0$, $f(\vec{q},t_0)$ describes an out of equilibrium situation, we can compute the value of these screening masses assuming the distribution function can be described by the parton model result for minijets. We note that to compute the second term on the right-hand side of Eqs. (29) and (32) we need to know the form of $[f(q_t,q_z)]_{q_t=0}$ and its behavior at RHIC and LHC. In this paper we are considering the minijet distribution function which are computed by using perturbative QCD (PQCD) applicable above $q_t=1(2)$ GeV at RHIC (LHC) which are obtained by saturation arguments as studied by several authors [23]. We mention here that PQCD is not applicable for small $q_t$, for example below 1 (2) GeV at RHIC (LHC). If one calculates the PQCD minijet production, the $q_t$ distribution behaves as $\propto q_t^{-\alpha}$ where $\alpha\sim 4$ for high $q_t$ and $\sim 2$ for low $q_t$. If one applies PQCD at small $q_t$, the distribution function $f(q_t,q_z)$ is singular at $q_t=0$. However, for very low $q_t$, PQCD formulas are not applicable and hence it is not obvious that distribution will be singular at $q_t=0$ at RHIC and LHC. For $q_t=0$ the only computation available at the moment is from the McLerran-Venugopalan model [24] where it is shown that at $q_t=0$ the gluon distribution behaves as a constant with respect to $q_t$ and does not behave as $q_t^{-\alpha}$. In this case we may assume that the gluon distribution does not diverge at $q_t=0$ in the realistic situation at RHIC and LHC. In such situations where $f(q_t=0,y,\phi)$ is not singular ($q_z=q_t\sinh y$ for gluon minijets) one can neglect the boundary term,

$$\begin{aligned}&[\sqrt{q_t^2+q_z^2}f(q_t,q_z,\phi)]\big|_{q_t=0}^{q_t=\infty}\\&=-[|q_z|f(q_t,q_z,\phi)]_{q_t=0}\\&=-[q_t|\sinh y|f(q_t,y,\phi)]_{q_t=0}=0\end{aligned} \tag{35}$$

since for massless minijets

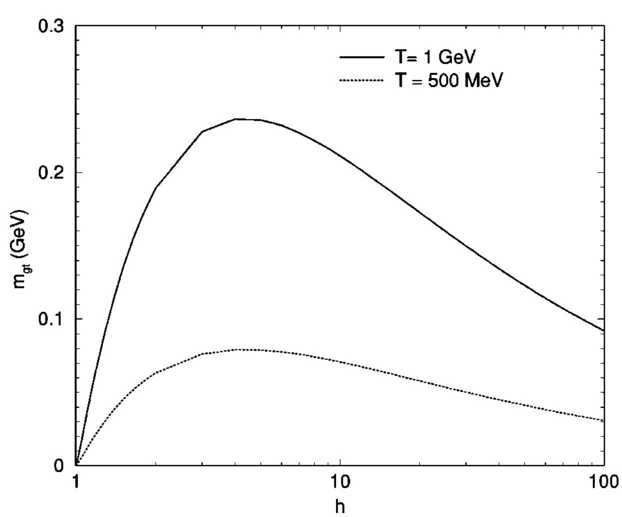


FIG. 2. The transverse component of the magnetic screening mass as obtained from Eq. (32) by using a nonisotropic distribution function of the form $f=1/(e^{\sqrt{q_t^2+hq_z^2}/T}-1)$ as a function of the nonisotropy parameter $h$. Note that for $h=1$ the distribution function becomes Bose-Einstein and hence the magnetic screening mass is found to be zero from Eq. (32).

$$q_z = q_t \sinh y = 0 \quad \text{when} \quad q_t = 0 \quad \text{for finite} \quad y. \tag{36}$$

Here $y$ is the momentum rapidity of the minijet parton. This boundary condition is *not* true in general, and in particular not true for a thermal distribution since a thermal distribution function $f_{eq} = 1/(e^{q_t \cosh y}/T - 1)$ is divergent at $q_t = 0$. However if the gluon distribution at $q_t = 0$ behaves as a constant at $q_t = 0$ at RHIC and LHC initial situations [24] then our vanishing boundary condition should be valid at RHIC and LHC. In any case a nonperturbative analysis of gluon distribution at $q_t = 0$ is beyond the scope of this paper. If the gluon distribution behavior at $q_t = 0$ is found to be divergent in any nonperturbative calculation unlike the case in [24] then the values reported in this paper might change. We have computed the Debye and magnetic screening masses in this paper above $q_t = 1$ (2) GeV at RHIC (LHC) which is similar to the calculations done by several authors for the Debye screening mass [25] where they have adopted similar cutoff values for the minijet momentum in their calculations.

With the above arguments and with the vanishing boundary conditions [Eqs. (35) and (36)] we get from Eq. (29), after changing to the rapidity variables $dq_z/|\vec{q}| = dy$,

$$m_{Dt}^2 = \frac{3\alpha_s}{\pi^2} \int dq_t q_t \int d\phi \int dy f(q_t, \phi, y), \tag{37}$$

where $f(q_t, \phi, y)$ is the nonisotropic gluon distribution function. For a cylindrically symmetric system we get

$$m_{Dt}^2 = \frac{6\alpha_s}{\pi} \int dq_t q_t \int dy f(q_t, y). \tag{38}$$

This is exactly the same equation used by several authors [2,26] in the context of minijet plasma equilibration in heavy-ion collisions at RHIC and LHC. Similarly using the same vanishing boundary condition [Eqs. (35) and (36)] we get for the magnetic screening mass from Eq. (32)

$$m_{gt}^2 = \frac{3\alpha_s}{\pi} \int dq_t q_t \int dy f(q_t, y), \tag{39}$$

for a cylindrically symmetric distribution function $f(q_t, y)$. It can be noted that in Eqs. (38) and (39) one should not use an equilibrium distribution function or any other distribution function which does not obey the vanishing boundary condition as stated in Eqs. (35) and (36).

For conditions pertinent to RHIC and LHC we use the minijet gluon distribution function to evaluate the Debye and magnetic screening masses. At high energy the minijet cross section can be calculated by using PQCD. The leading order minijet cross section is given by

$$\sigma_{jet} = \int dp_t \int dy_1 \int dy_2 \frac{2\pi p_t}{\hat{s}} \sum_{ijkl} x_1 f_{i/A}(x_1, p_t^2) \times x_2 f_{j/A}(x_2, p_t^2) \hat{\sigma}_{ij\to kl}(\hat{s}, \hat{t}, \hat{u}). \tag{40}$$

Here $x_1$ and $x_2$ are the light-cone momentum fractions carried by the partons $i$ and $j$ from the projectile and the target, respectively, $f$ are the bound-nucleon structure functions and $y_1$ and $y_2$ are the rapidities of the scattered partons. The symbols with carets refer to the parton-parton c.m. system. The $\hat{\sigma}_{ij\to kl}$ are the elementary PQCD parton cross sections. As we will be considering a gluon system we include the dominant gluon production cross sections at the partonic level which are given by

$$\hat{\sigma}_{gq\to gq} = \frac{\alpha_s^2}{\hat{s}} (\hat{s}^2 + \hat{u}^2) \left[ \frac{1}{\hat{t}^2} - \frac{4}{9\hat{s}\hat{u}} \right], \tag{41}$$

and

$$\hat{\sigma}_{gg\to gg} = \frac{9\alpha_s^2}{2\hat{s}} \left[ 3 - \frac{\hat{u}\hat{t}}{\hat{s}^2} - \frac{\hat{u}\hat{s}}{\hat{t}^2} - \frac{\hat{s}\hat{t}}{\hat{u}^2} \right]. \tag{42}$$

Here $\alpha_s$ is the strong coupling constant and

$$\hat{s} = x_1 x_2 s = 4 p_t^2 \cosh^2\left( \frac{y_1 - y_2}{2} \right). \tag{43}$$

The rapidities $y_1$, $y_2$ and the momentum fractions $x_1$, $x_2$ are related by

$$x_1 = p_t (e^{y_1} + e^{y_2})/\sqrt{s},$$

$$x_2 = p_t (e^{-y_1} + e^{-y_2})/\sqrt{s}. \tag{44}$$

The limits of integrations are given by

$$p_{min} \leqslant p_t \leqslant \frac{\sqrt{s}}{2\cosh y_1},$$

$$-\ln(\sqrt{s}/p_t - e^{-y_1}) \leqslant y_2 \leqslant \ln(\sqrt{s}/p_t - e^{y_1}), \tag{45}$$

with

$$|y_1| \leqslant \ln(\sqrt{s}/2p_{min} + \sqrt{s/4p_{min}^2 - 1}). \tag{46}$$

In the above equations $p_{min}$ is the minimum transverse momentum above which minijet production is computed by using PQCD. We multiply the above minijet cross sections by a $K$ factor $K = 2$ to account for the higher order $O(\alpha_s^3)$ contributions. The minimum transverse momentum above which the minijets are computed via PQCD is of the order of $p_{min} \sim 1$ GeV at RHIC and $\sim 2$ GeV at LHC [23]. These values are energy dependent and are obtained from the saturation arguments. We take $p_{min} = 1$ GeV at RHIC and 2 GeV at LHC for our computations. The minijet cross section [Eq. (40)] can be related to the total number of partons ($N$) by

$$N^{jet} = T(0) \quad \sigma_{jet}, \tag{47}$$

where $T(0) = 9A^2/8\pi R_A^2$ is the total number of nucleon-nucleon collisions per unit area for central collisions [27]. Here $R_A = 1.1 A^{1/3}$ is the nuclear radius. A rough estimate of the initial volume in which these initial partons are formed at RHIC and LHC can be given by $V_0 = \pi R_A^2 \tau_0$, where the partons are assumed to be spread by a length $\tau_0 = 1/p_{min}$. Assuming that the partons are uniformly distributed in the coordinate space (but nonisotropic in momentum space) we can easily extract a phase-space gluon distribution function of the gluon from the total number of gluon minijets from Eq. (47). The initial distribution function of the gluon is then given by

$$f(p_t, y_1) = \frac{1}{\pi R_A^2 \tau_0} dN^{jet}/d^3p \tag{48}$$

where

$$d^3p = d^2p_t dp_z = p_t d^2p_t \cosh y_1 dy_1. \tag{49}$$

Using the above minijet initial gluon distribution function in Eq. (38) and Eq. (39) we get

$$m_{Dt}^2 = \frac{T(0)}{\pi^2 R_A^2 \tau_0} 6 \;\; K\alpha_s \int dp_t \int dy_1 \int dy_2 \frac{1}{\hat{s}\cosh y_1} \sum_{ijkl} x_1 f_{i/A}(x_1, p_t^2) x_2 f_{j/A}(x_2, p_t^2) \hat{\sigma}_{ij\to kl}(\hat{s}, \hat{t}, \hat{u}), \tag{50}$$

for the Debye screening mass and

$$m_{gt}^2 = \frac{T(0)}{\pi^2 R_A^2 \tau_0} 3 \;\; K\alpha_s \int dp_t \int dy_1 \int dy_2 \frac{1}{\hat{s}\cosh y_1} \sum_{ijkl} x_1 f_{i/A}(x_1, p_t^2) x_2 f_{j/A}(x_2, p_t^2) \hat{\sigma}_{ij\to kl}(\hat{s}, \hat{t}, \hat{u}), \tag{51}$$

for the magnetic screening mass of the gluon at the one loop level. Note that in the above equation $\alpha_s$ occurs outside the $p_t$ integration and hence a scale has to be defined, at which this coupling constant has to be determined. For this purpose we take $\alpha_s$ as $\alpha_s(\langle p_t^2\rangle)$ where the momentum scale $\langle p_t^2\rangle$ is defined by

$$\langle p_t^2\rangle = \frac{1}{\sigma^{jet}} \int dp_t p_t^2 \int dy_1 \int dy_2 \frac{2\pi p_t}{s} \sum_{ijkl} x_1 f_{i/A}(x_1, p_t^2) x_2 f_{j/A}(x_2, p_t^2) \hat{\sigma}_{ij\to kl}(\hat{s}, \hat{t}, \hat{u}), \tag{52}$$

where $\sigma^{jet}$ is defined by Eq. (40).

In this paper we will be using both Glück-Reya-Vogti 1998 (GRV98) [28] and CTEQ6M [29] parametrizations for the gluon and quark structure functions inside a free proton with Eskola-Kolhinen-Ruiskanen-Sagado 1998 (EKRS98) [30] parametrizations for the nuclear modifications. In Fig. 3 we present the results of the initial gluon distribution function [see Eq. (48)] at RHIC as a function of the transverse momentum of the gluon for different values of the rapidities.

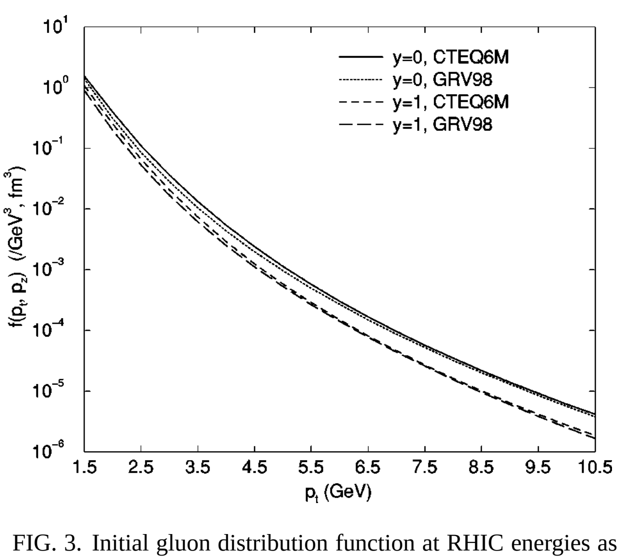


FIG. 3. Initial gluon distribution function at RHIC energies as a function of $p_t$.

The rapidity $y$ is related to the longitudinal momentum $p_z$ via $p_z = p_t \sinh y$.

We present the longitudinal momentum distribution of the initial gluon minijet distribution function at RHIC in Fig. 4 for different values of $p_t$.

Using these gluon minijet distribution functions in Eqs. (50) and (51) we get for RHIC

$$m_{Dt} = 116 \;\; \text{MeV} \quad \text{and} \quad m_{gt} = 82 \;\; \text{MeV} \tag{53}$$

and for LHC

$$m_{Dt} = 150 \;\; \text{MeV} \quad \text{and} \quad m_{gt} = 105 \;\; \text{MeV} \tag{54}$$

by using GRV98 structure functions along with EKRS98. The coupling constant $\alpha_s(\langle p_t^2\rangle)$ is found to be 0.287 at RHIC and 0.214 at LHC. If higher order contribution to the minijet production would have not been taken into account then our results of screening mass would have been $\sqrt{K(=2)}$ times less than the above values. The above masses may be lower bounds to the actual values as we have used a lower transverse momentum cutoff for minijets in order for PQCD to be applicable. However, the gluon distribution may be dominant at lower $p_t$ [24] and hence the magnitude of the screening mass may increase if one can include the soft partons into the gluon distribution function. The values we reported in this paper are for gluon minijet distribution functions at RHIC and LHC with $p_{min}$ greater than 1 and 2 GeV respectively.

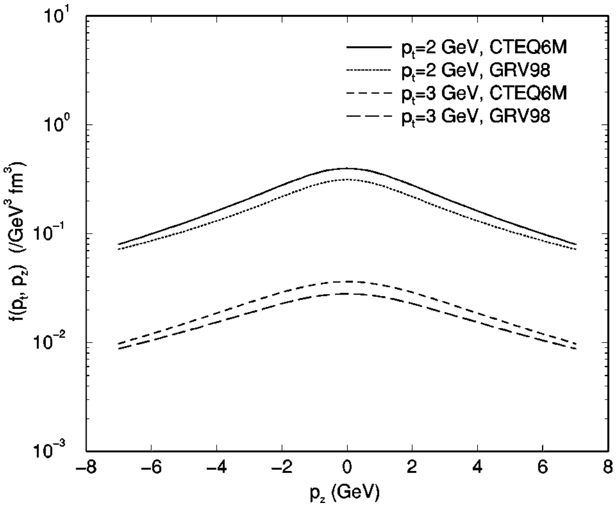


FIG. 4. Initial gluon distribution function at RHIC energies as a function of $p_z$.

Let us now look at the equilibrium situation. Note that at one loop level we get [see Eq. (26)] $m_D^2 = g^2 T^2$ and $m_g^2 = 0$ in equilibrium. Since the one loop magnetic mass is zero in equilibrium we will compare our results with the magnetic mass which is obtained by using nonperturbative methods. The magnetic mass obtained by using nonperturbative methods in equilibrium is given by $m_g^2 = \frac{3}{2}(0.255 g^2 T)^2$, see [5,31]. Assuming a temperature of about 500 MeV at RHIC and by using the coupling constant value $\alpha_s = 0.287$ at RHIC [see above) we get $m_D = gT = 950$ MeV and $m_g = \sqrt{\frac{3}{2}}(0.255 g^2 T) = 563$ MeV. Assuming $T = 1000$ GeV at LHC and using the LHC coupling constant $\alpha_s = 0.214$ we obtain $m_D = 1.639$ GeV and $m_g = 840$ GeV. In obtaining these masses, one has integrated over all momentum ranges of the equilibrium distribution functions. For example, if one uses a Bose-Einstein distribution function in Eq. (24) and then integrates from $(p_{min} \rightarrow \sqrt{s}/2)$ then we obtain $m_D = 486$ GeV at RHIC for T=500 GeV and $\alpha_s = 0.287$. Similarly for LHC one obtains $m_D = 840$ GeV for T=1 GeV and $\alpha_s = 0.214$.

Note that these values are of the same order as that obtained by using the nonequilibrium distribution functions at RHIC and LHC. Since the gluon distribution function may be dominant at lower $p_t$ the magnitude of the screening mass might increase if one can include the soft partons into the gluon distribution function [9,10,32–36]. The values we reported in this paper are for gluon minijet distribution functions at RHIC and LHC with $p_{min}$ greater than 1 and 2 GeV respectively. Note that due to the asymmetry we have computed a specific component ($\hat{p}$ in the transverse direction) of the Debye ($m_{Dt}$) and magnetic ($m_{gt}$) screening mass. If one computes the values in all directions their values may be even higher. Similar situations hold for magnetic screening masses at RHIC and LHC. As the magnetic mass is a nonperturbative calculation at equilibrium and ours is a one loop calculation at nonequilibrium, we expect that a nonperturbative nonequilibrium calculation might give a higher magnetic screening mass. The argument is similar to the study of a nonperturbative calculation for the Debye screening mass at finite temperature [37].

To summarize, we have applied the closed-time path formalism to nonequilibrium situations in QCD expected at RHIC and LHC energies to study the infrared behavior of the one loop gluon self-energy. We have followed a frozen ghost formalism where the initial density of states consists of physical gluons and the ghost is only present in the vacuum level. In the infrared limit of the gluon self-energy we obtain a nonvanishing magnetic screening mass of the gluon at the one loop level for nonisotropic gluon distribution functions with the assumption that the distribution function of the gluon is not divergent at zero transverse momentum. At RHIC and LHC we assumed that the gluon distribution is not divergent at $q_t = 0$ which is supported by the computation done in [24]. With this approximation we then applied PQCD above $q_t = 1$ (2) GeV at RHIC (LHC) and obtain a reasonable initial nonequilibrium gluon-minijet distribution function. Using this nonisotropic gluon minijet distribution function above $q_t = 1$ (2) GeV at RHIC (LHC) we predicted the values of the magnetic and Debye screening masses at the initial time [38].

We thank Tanmoy Bhattacharya, Larry McLerran, Emil Mottola, E. V. Shuryak and Raju Venugopalan for useful discussions.

[1] X.N. Wang, Phys. Rep. **280**, 287 (1997); X.N. Wang and Miklos Gyulassy, Phys. Rev. D **44**, 3501 (1991); K.J. Eskola and K. Kajantie, Z. Phys. C **75**, 515 (1997); A. Krasnitz and R. Venugopalan, Phys. Rev. Lett. **84**, 4309 (2000); K. Geiger, Phys. Rep. **258**, 237 (1995); K. Geiger and B. Muller, Nucl. Phys. **B369**, 600 (1992); N. Hammon, H. Stoecker, and W. Greiner, Phys. Rev. C **61**, 014901 (2000).

[2] G.C. Nayak, A. Dumitru, L. McLerran, and W. Greiner, Nucl. Phys. **A687**, 457 (2001).

[3] R. Baier, A.H. Mueller, D. Schiff, and D.T. Son, Phys. Lett. B **502**, 51 (2001); A.H. Mueller, *ibid.* **475**, 220 (2000).

[4] K. Geiger, Phys. Rep. **280**, 237 (1995); K. Geiger and J.I. Kapusta, Phys. Rev. D **47**, 4905 (1993).

[5] H. Heiselberg and X.N. Wang, Nucl. Phys. **B462**, 389 (1996).

[6] S.H.M. Wong, Phys. Rev. C **54**, 2588 (1996); **56**, 1075 (1997).

[7] M. Gyulassy, Y. Pang, and B. Zhang, Nucl. Phys. **A626**, 999 (1997); B. Zhang, Comput. Phys. Commun. **109**, 193 (1998).

[8] A. Hosoya and K. Kajantie, Nucl. Phys. **B250**, 666 (1985).

[9] R.S. Bhalerao and G.C. Nayak, Phys. Rev. C **61**, 054907 (2000).

[10] G.C. Nayak and V. Ravishankar, Phys. Rev. D **55**, 6877 (1997); Phys. Rev. C **58**, 356 (1998).

[11] R.D. Pisarski, Phys. Rev. D **47**, 5589 (1993); E. Braaten and R.D. Pisarski, Nucl. Phys. **B339**, 310 (1990); T. Altherr, Phys. Lett. B **341**, 325 (1995); R. Baier, M. Dirks, K. Redlich, and D. Schiff, Phys. Rev. D **56**, 2548 (1997), and references therein.

[12] J. Schwinger, J. Math. Phys. **2**, 407 (1961); P.M. Bakshi and K.T. Mahanthappa, *ibid.* **4**, 1 (1963); **4**, 12 (1963); L.V. Keldysh, Zh. Éksp. Teor. Fiz. **47**, 1515 (1964) [Sov. Phys. JETP **20**, 1018 (1965)]; G. Zhou, Z. Su, B. Hao, and L. Yu, Phys. Rep. **118**, 1 (1985).
[13] For example, see M.H. Thoma, 10th Jyvaskyla Summer School, Jyvaskyla, Finland, hep-ph/0010164; S. Mrowczynski and M.H. Thoma, Phys. Rev. D **62**, 036011 (2000).
[14] A.K. Rebhan, Phys. Rev. D **48**, R3967 (1993).
[15] C.-W. Kao, G.C. Nayak, and W. Greiner, Phys. Rev. D **66**, 034017 (2002).
[16] N.P. Landsman and Ch.G. van Weert, Phys. Rep. **145**, 141 (1987).
[17] H.A. Weldon, Phys. Rev. D **26**, 1394 (1982), and references therein.
[18] P.V. Landshoff and A. Rebhan, Nucl. Phys. **B383**, 607 (1992); **B406**, 517(E) (1993).
[19] M. D'Attanasio and M. Pietroni, Nucl. Phys. **B498**, 443 (1997).
[20] See, for example, T.S. Biro, B. Muller, and X.N. Wang, Phys. Lett. B **283**, 171 (1992); H. Satz and D. Srivastava, *ibid.* **475**, 225 (2000); T.S. Biro, Int. J. Mod. Phys. B **1**, 39 (1992), and references therein.
[21] J.-P. Blaizot, E. Iancu, and R.R. Parwani, Phys. Rev. D **52**, 2543 (1995).
[22] F. Cooper, C.-W. Kao, and G.C. Nayak, hep-ph/0207370.
[23] A.H. Mueller, Nucl. Phys. **B572**, 227 (2000); K.J. Eskola, K. Kajantie, P.V. Ruuskanen, and K. Tuominen, *ibid.* **B570**, 379 (2000).
[24] A. Krasnitz, Y. Nara, and R. Venugopalan, Phys. Rev. Lett. **87**, 192302 (2001).
[25] K.J. Eskola, B. Muller, and X.-N. Wang, Phys. Lett. B **374**, 20 (1996), and references therein.
[26] J. Bjoraker and R. Venugopalan, Phys. Rev. C **63**, 024609 (2001); J. Serreau and D. Schiff, J. High Energy Phys. **11**, 039 (2001); R. Baier, A.H. Mueller, D. Schiff, and D.T. Son, Phys. Lett. B **502**, 51 (2001).
[27] K.J. Eskola, K. Kajantie, and J. Lindfors, Nucl. Phys. **B323**, 37 (1989).
[28] M. Glück, E. Reya, and A. Vogt, Eur. Phys. J. C **5**, 461 (1998).
[29] J. Pumplin, D.R. Stump, J. Huston, H.L. Lai, P. Nadolsky, and W.K. Tung, J. High Energy Phys. **07**, 012 (2002).
[30] K.J. Eskola, V.J. Kolhinen, and P.V. Ruuskanen, Nucl. Phys. **B535**, 351 (1998); K.J. Eskola, V.J. Kolhinen, and C.A. Sagado, Eur. Phys. J. C **9**, 61 (1999).
[31] See T.S. Biro and B. Muller, Nucl. Phys. **A561**, 477 (1993), and references therein; J. Ruppert, G.C. Nayak, D.D. Dietrich, H. Stoecker, and W. Greiner, Phys. Lett. B **520**, 233 (2001).
[32] Y. Kluger, J.M. Eisenberg, B. Svetitsky, F. Cooper, and E. Motolla, Phys. Rev. Lett. **67**, 2427 (1991); F. Cooper, J.M. Eisenberg, Y. Kluger, E. Motolla, and B. Svetitsky, Phys. Rev. D **48**, 190 (1993); F. Cooper and E. Motolla, *ibid.* **36**, 3114 (1987); **40**, 456 (1989); T.S. Biro, H.B. Nielsen, and J. Knoll, Nucl. Phys. **B245**, 449 (1984); M. Herrmann and J. Knoll, Phys. Lett. B **234**, 437 (1990); D. Boyanovsky, H.J. de Vega, R. Holman, D.s. Lee, and A. Singh, Phys. Rev. D **51**, 4419 (1995); H. Gies, *ibid.* **61**, 085021 (2000).
[33] L. McLerran and R. Venugopalan, Phys. Rev. D **49**, 2233 (1994); **49**, 3352 (1994); Yu. Kovchegov and A.H. Mueller, Nucl. Phys. **B529**, 451 (1998); A. Kovner, L. McLerran, and H. Weigert, Phys. Rev. D **52**, 3809 (1998), **52**, 6231 (1998); Y.V. Kovchegov, E. Levin, and L. McLerran, Phys. Rev. C **63**, 024903 (2001).
[34] D.D. Dietrich, G.C. Nayak, and W. Greiner, Phys. Rev. D **64**, 074006 (2001); hep-ph/0009178; J. Phys. G **28**, 2001 (2002); G.C. Nayak, D.D. Dietrich, and W. Greiner, Rostock 2000/Trento 2001, Exploring Quark Matter 71-78, hep-ph/0104030.
[35] C.D. Roberts and S.M. Schmidt, Prog. Part. Nucl. Phys. **45**, 1 (2000); V. Vinik *et al.*, Eur. Phys. J. C **22**, 341 (2001); J.C.R. Bloch, C.D. Roberts, and S.M. Schmidt, Phys. Rev. D **61**, 117502 (2000); J.C.R. Bloch, *et al.*, *ibid.* **64**, 116011 (1999).
[36] J.-P. Blaizot and E. Iancu, Phys. Rep. **359**, 355 (2002); Nucl. Phys. **B570**, 326 (2000); *ibid.* **B417**, 608 (1994).
[37] K. Kajantie *et al.*, Phys. Rev. Lett. **79**, 3130 (1997).
[38] K.J. Eskola, B. Muller, and X.-N. Wang, Phys. Lett. B **374**, 20 (1996).